PHYSICAL REVIEW B **89**, 161111(R) (2014)

High-harmonic generation by nonlinear resonant excitation of surface plasmon modes in metallic nanoparticles

Jérôme Hurst
Institut de Physique et Chimie des Matériaux de Strasbourg and Labex NIE, Université de Strasbourg, CNRS UMR 7504 BP 43 - F-67034 Strasbourg Cedex 2, France

Fernando Haas*
Departamento de Física, Universidade Federal do Paraná, 81531-990, Curitiba, Paraná, Brazil

Giovanni Manfredi† and Paul-Antoine Hervieux
Institut de Physique et Chimie des Matériaux de Strasbourg and Labex NIE, Université de Strasbourg, CNRS UMR 7504 BP 43 - F-67034 Strasbourg Cedex 2, France

(Received 14 January 2014; published 18 April 2014)

The nonlinear electron dynamics in metallic nanoparticles is studied using a hydrodynamic model that incorporates most quantum many-body features, including spill-out and nonlocal effects as well as electron exchange and correlations. We show that, by irradiating the nanoparticle with a chirped laser pulse of modest intensity (autoresonance), it is possible to drive the electron dynamics far into the nonlinear regime, leading to enhanced energy absorption and complete ionization of the nanoparticle on a time scale of the order of 100 fs. The accompanying radiated power spectrum is rich in high-order harmonics.

DOI: 10.1103/PhysRevB.89.161111 PACS number(s): 78.67.Bf, 73.22.Lp, 73.63.−b, 78.66.Bz

Introduction. Metallic nanoparticles [1] are mesoscopic systems composed of a relatively small number of atoms, typically between a few tens and several millions. With properties that are intermediate between those of molecules and bulk solids, metallic nanoparticles present an intrinsic fundamental interest as large objects that still display quantum features [2–5]. Their potential technological applications are far reaching, ranging from the recent field of nanophotonics [6,7] to physical chemistry [8], and even biology and medicine [9,10].

Experimentally, the electron dynamics in a metallic nanoparticle can be probed with great precision using ultrafast spectroscopy techniques in the femtosecond regime [11,12]. From the theoretical point of view, the linear response has been the object of intense investigations in the past decades [13,14]. In contrast, the nonlinear regime is much harder to assess using many-body approaches such as the time-dependent density functional theory (DFT) [15,16] or Wigner function methods [17,18]. A possible alternative relies on the use of macroscopic models based on a set of quantum hydrodynamic (QHD) equations [19,20], which were successfully used in the past to model the electron dynamics in molecular systems [21], metallic nanoparticles [22–25], thin films [26], and semiconductor quantum wells [27].

A further degree of simplification can be achieved by means of a variational approach [24], which expresses the QHD model in terms of a Lagrangian function. By postulating a reasonable ansatz for the electron density, it is possible to obtain a set of ordinary differential equations for some macroscopic quantities, such as the center of mass and the radial extension of the electron gas.

Using this approach, we will study the dynamics of collective electron modes (surface plasmons) excited with laser pulses in the visible range. Using chirped pulses with slowly varying frequency (autoresonance), it is possible to drive the plasmon mode far into the nonlinear regime, leading to the emission of electromagnetic radiation with a power spectrum rich in high-order harmonics.

The autoresonant technique [28–32] is very flexible and efficient—the required laser intensities are modest ($\sim 10^{10}$ W/cm^2) and no feedback mechanism is needed to match the driving frequency with the oscillator frequency. Further, this technique is expected to work even in the case of nanoparticles of unequal sizes, which is the most common situation in the experiments [33]. Thus the electron response of an assembly of metallic nanoparticles could be excited well into the nonlinear regime, leading to a dramatic increase of the absorbed energy.

Quantum hydrodynamic model. In order to study the electron dynamics in a metal nanoparticle, we make use of a QHD model [19,20] that governs the evolution of the electron density $n(\mathbf{r},t)$, mean velocity $\mathbf{u}(\mathbf{r},t)$, and pressure $P(\mathbf{r},t)$. The QHD equations read as (all quantities are expressed in atomic units unless otherwise stated)

$$\frac{\partial n}{\partial t} + \nabla \cdot (n\mathbf{u}) = 0, \tag{1}$$

$$\frac{\partial \mathbf{u}}{\partial t} + \mathbf{u} \cdot \nabla \mathbf{u} = \nabla V_H - \nabla V_X - \frac{\nabla P}{n} + \frac{1}{2}\nabla\left(\frac{\nabla^2\sqrt{n}}{\sqrt{n}}\right). \tag{2}$$

Equation (1) is the continuity equation representing conservation of mass, while Eq. (2) is an Euler equation that provides the evolution of the mean velocity under the action of the forces that appear on the right-hand side. The mean-field part of the electron-electron interactions is taken into account by the Hartree potential V_H, which obeys Poisson's equation:

*ferhaas@fisica.ufpr.br; Present address: Physics Institute, Universidade Federal do Rio Grande do Sul, CEP 91501-970, Porto Alegre, RS, Brazil.
†giovanni.manfredi@ipcms.unistra.fr

$\nabla^2 V_H = 4\pi(n - n_i)$, where n_i is the ion density. The potential V_X represents the exchange interaction:

$$V_X = -\frac{(3\pi^2)^{1/3}}{\pi} n^{1/3} - \frac{4\beta}{3}\frac{(\nabla n)^2}{n^{7/3}} + 2\beta\frac{(\nabla n)^2}{n^{4/3}}, \qquad (3)$$

where the first term is the local density approximation (LDA) and the other two terms constitute a gradient correction. The prefactor β is a free parameter that we set equal to $\beta = 0.005$, which is a best fit frequently used in atomic-structure calculations [34]. For P, we use the expression of the Fermi pressure for a zero-temperature electron gas: $P = (3\pi^2)^{2/3} n^{5/3}/5$. The last term (Bohm potential) takes into account quantum diffraction effects. Note that the Bohm potential and the exchange gradient correction are nonlocal effects. The details of the derivation of the QHD model can be found in Ref. [20].

Correlation effects have been ignored so far, but will be included later in the form of a density-dependent correlation potential $V_C[n(\mathbf{r},t)]$. In practice, they yield only minimal corrections.

We shall consider spherical gold nanoparticles of radius R, composed of N electrons and N singly ionized ions. The ions are fixed and form a homogeneous positive charge density equal to $n_i = n_0 = (\frac{4}{3}\pi r_s^3)^{-1}$ inside the nanoparticle, and zero outside, where $r_s = 3.01$ a.u. is the Wigner-Seitz radius of gold.

Variational method. The hydrodynamic model (1) and (2) can be derived from the Lagrangian density [24,27]

$$\mathcal{L} = n\left[\frac{\partial S}{\partial t} + \frac{(\nabla S)^2}{2}\right] + \frac{(\nabla n)^2}{8n} + \frac{3}{10}(3\pi^2)^{2/3} n^{5/3} - \frac{3}{4\pi}(3\pi^2)^{1/3} n^{4/3} - \beta\frac{(\nabla n)^2}{n^{4/3}} - \frac{(\nabla V_H)^2}{8\pi} + (n_i - n)V_H. \qquad (4)$$

This Lagrangian density depends on three scalar fields, namely the density $n(\mathbf{r},t)$, the Hartree potential $V_H(\mathbf{r},t)$, and the phase function $S(\mathbf{r},t)$, which is related to the mean velocity $\mathbf{u}$ by the expression $\mathbf{u} = \nabla S$.

Our purpose is to derive, using a variational approach, a set of differential equations for a small number of macroscopic quantities that characterize the electron density profile [24,27]. This can be achieved by positing a reasonable ansatz for the above scalar fields and integrating the Lagrangian density (4) over space.

We start with the electron density, which, to a good approximation, is flat and equal to n_0 inside the nanoparticle ($r \leqslant R$) and decreases smoothly to zero near $r = R$ (see Fig. 1). Some electrons are present beyond the nominal radius R, an effect know as the spill-out. In order to reproduce qualitatively such a density profile, we assume that the electron density has the following form:

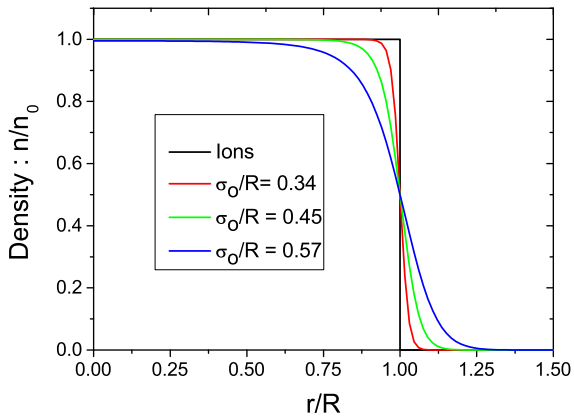

FIG. 1. (Color online) Schematic view of the ion and electron densities according to (5) for different values of the spill-out parameter σ_0.

$$n(r,t) = A\left\{1 + \exp\left[\left(\frac{s}{\sigma(t)}\right)^3 - \left(\frac{R}{\sigma_0}\right)^3\right]\right\}^{-1}, \qquad (5)$$

where A is chosen to satisfy the normalization condition $\int n\, d\mathbf{r} = N$, and s is a displaced radial coordinate defined as $s(t) = \sqrt{x^2 + y^2 + [z - d(t)]^2}$. In the above expression, we introduced two macroscopic dynamical variables, namely (i) the center of mass of the electron gas $d(t)$, which can be displaced along the z axis, and (ii) the thickness of the spill-out effect $\sigma(t)$. At equilibrium $d = 0$ and $\sigma = \sigma_0$. Of course, the above ansatz precludes the possibility to observe higher-order modes (quadrupole, octupole). Although these modes may be excited nonlinearly, we restrict our analysis to the lower-order dipole and monopole (breathing) modes.

Making use of Eq. (5) together with the continuity and Poisson equations, it is possible to obtain exact expressions for the two other fields, S and V_H, as a function of the dynamical variables $d(t)$ and $\sigma(t)$. With these expressions, we can integrate the Lagrangian density (4) over space in order to obtain the Lagrangian function $L(d,\sigma,\dot{d},\dot{\sigma})$, where a dot denotes differentiation with respect to time. The integration can be performed analytically only by expanding the Lagrangian in a power series in the variable d/R. We obtain, up to order $O(d^5/R^5)$,

$$L = \frac{-1}{N}\int \mathcal{L}\, d\mathbf{r} = \frac{M(a)\dot{\sigma}^2}{2} - U(\sigma) + \frac{\dot{d}^2}{2} - \frac{\Omega_d^2(\sigma) d^2}{2} + K(\sigma) d^4, \qquad (6)$$

where $a = \exp(-R^3/\sigma_0^3)$ and $M(a) > 0$ is a fictitious mass. The functions $\Omega_d(\sigma)$ and $K(\sigma)$, which are both positive definite, correspond respectively to the second- and fourth-order terms in the development of the electron-ion interaction energy. The pseudopotential $U(\sigma)$ is a complicated function expressed as the sum of many integral terms, which possesses a single minimum located at σ_0. All the details of the calculations leading to Eq. (6) are provided in the Supplemental Material [35].

Using the Euler-Lagrange equations for L, we obtain the following coupled equations of motion:

$$\ddot{\sigma} = \frac{1}{M(a)}\left\{ -\frac{dU(\sigma)}{d\sigma} + \frac{3Nd^2}{2\sigma^4 \ln(1+1/a)} \frac{1}{1+a\,\exp(R^3/\sigma^3)} - \frac{27NRa\,\exp(R^3/\sigma^3)d^4}{40\,\ln(1+1/a)\sigma^{10}} \frac{[1-a\,\exp(R^3/\sigma^3)]R^3 + 2[1+a\,\exp(R^3/\sigma^3)]\sigma^3}{[1+a\,\exp(R^3/\sigma^3)]^3} \right\}, \tag{7}$$

$$\ddot{d} = -\Omega_d^2(\sigma)d + 4K(\sigma)d^3, \tag{8}$$

which describe respectively the breathing and dipole oscillations.

In summary, we have reduced the formidable problem of the quantum electron dynamics in a metallic nanoparticle to a simple set of two coupled differential equations, which can be easily solved even for large systems containing many electrons, where DFT methods are too costly. No assumptions of linearity were made so far, so that Eqs. (7) and (8) can be used to study the nonlinear response (as long as d is not too large). Further, compared to simple "rigid sphere models" [36], our approach incorporates many more effects, including quantum nonlocality, spill-out, exchange, and (as shown later) correlations [37].

Ground state and linear response. In order to validate the above model, we first present an analysis of the ground state and linear response of the system, for which well-established results, both theoretical and experimental, already exist. The ground state of the system is obtained by setting the time derivatives equal to zero in Eqs. (7) and (8). Equation (8) is satisfied automatically for $d = 0$ (i.e., the centers of mass of the ions and the electrons should coincide). Setting $d = 0$ in Eq. (7), the stable equilibrium is the value σ_0 that minimizes the pseudopotential $U(\sigma)$. For instance, for a gold nanoparticle with $N = 200$, we find a diameter $2R = 2r_s N^{1/3} = 1.86$ nm and spill-out width $\sigma_0 = 0.44$ nm (more values are given in the Supplemental Material [35]).

In the linear response regime, one can identify two electronic modes, corresponding to oscillations of $\sigma(t)$ (breathing mode) and oscillations of $d(t)$ (dipole, or surface plasmon, mode). We first consider the breathing mode. Setting $d = 0$ in Eq. (7) and expanding $U(\sigma)$ around σ_0 up to first order, we obtain $M(a)\ddot{\sigma} = -U''(\sigma_0)(\sigma - \sigma_0)$. The linear breathing frequency is therefore $\Omega_b = \sqrt{U''(\sigma_0)/M(a)}$, which can be easily evaluated numerically.

For the dipole mode, assuming that $\sigma = \sigma_0$ and $d \ll R$, Eq. (8) yields immediately the linear dipole frequency $\Omega_d(\sigma_0)$. For large nanoparticles, the latter tends to the bulk Mie frequency [1,38] $\omega_{\rm Mie} = \omega_p/\sqrt{3}$ (where $\omega_p = \sqrt{4\pi n_0}$ is the plasmon frequency), as can be checked directly by taking the limit $R/\sigma_0 \to \infty$.

In general, both the dipole and breather frequencies should depend on the size of the nanoparticle in the following fashion [39–41]: $\Omega_{d,b}(N) = \Omega_\infty(1 - k_{d,b}N^{-1/3})$, where $k_{d,b}$ are positive constants, and Ω_∞ is equal to $\omega_{\rm Mie}$ for the dipole mode and to ω_p for the breathing mode. Our model reproduces very well these scalings, as can be seen from Fig. 2. The extrapolation at $N \to \infty$ gives the Mie or plasmon frequency for the bulk.

Correlations. Electron correlations can be introduced through an appropriate functional of the density. Here, we use the functional proposed by Brey *et al.* [42], which yields the following correlation potential: $V_C = -\gamma\,\ln[1 + \delta n^{1/3}]$, with $\gamma = 0.033\,49$ and $\delta = 18.376$. This potential can be included in our Lagrangian formalism (details are given in the Supplemental Material [35]). For all the cases we studied, the effect of the correlations was almost negligible, as can be seen from Fig. 2. Indeed, a quick estimate shows that the ratio between the exchange (LDA) and the correlation potentials is very small, $V_C/V_{X,\rm LDA} \approx 0.084$. This is also in agreement with early results obtained with DFT and Hartree-Fock methods [43].

Nonlinear response and autoresonant excitation. We now turn our attention to the excitation of the electron dynamics by means of electromagnetic waves (laser pulses). First, it should be noted that the relevant linear frequencies computed in the preceding section are of the order of a few electron volts. For instance, for $N = 200$, $\Omega_d = 0.1841$ a.u. $= 5$ eV. These frequencies fall within the visible or near-ultraviolet (UV) spectrum, which is encouraging since visible and near-UV lasers are commonly employed in ultrafast optics experiments. For such lasers, the wavelength is several hundred nanometers long, i.e., much larger than the size of a typical metallic nanoparticle. This means that the laser pulse can only couple to the dipole mode.

We assume that the electron gas in the nanoparticle is excited via an oscillating electric field directed along the z

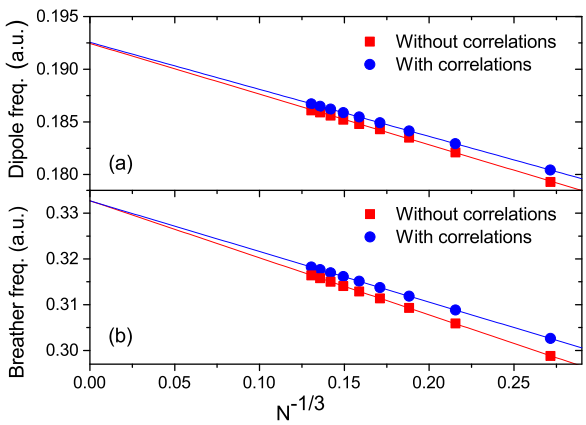

FIG. 2. (Color online) Linear dipole (a) and breathing (b) frequencies for gold nanoparticles as a function of $N^{-1/3}$. Blue circles and red squares represent respectively the results with and without correlations. The straight lines are linear fits.

axis, $\mathbf{E} = E_z(t)\mathbf{e}_z$. The effect of the laser can be included by adding a term $E_z d$ to the Lagrangian L. If the laser frequency is equal to the dipole frequency, the excitation is resonant: the dipole oscillations grow initially, but then decrease after some time. This is because the effective dipole force is not harmonic and the resonant frequency actually depends on the amplitude of the oscillations.

The above limitation can be overcome by resorting to *autoresonant* excitation [28]. Basically, autoresonance occurs when a classical nonlinear oscillator is externally excited by an oscillating field with slowly varying frequency. In our notation, $E_z(t) = E_0 \cos\left[\Omega_d(t-t_0) + \alpha(t-t_0)^2\right]$, where E_0 is the excitation amplitude, t_0 is the time when the instantaneous frequency of the laser is equal to the linear frequency of the dipole mode, and α is the rate of variation of the laser frequency. For $|\alpha| \ll \Omega_d^2$ and E_0 above a certain threshold, the instantaneous oscillator frequency becomes "locked" to the instantaneous excitation frequency, so that the resonance condition is always satisfied. In that case, the amplitude of the oscillations grows indefinitely and without saturation, until of course some other effect kicks in. The threshold behaves as $E_0^{\text{th}} \sim |\alpha|^{3/4}$, so that the amplitude can be arbitrarily small provided that the external frequency varies slowly enough [28].

In Fig. 3, we display the results of an autoresonant excitation of the electron gas, for two realistic (but still very modest) [44] values of the laser intensity $I_0 = \frac{1}{2}c\varepsilon_0|E_0|^2$ that are either below or above the autoresonant threshold. For an intensity $I_0 = 4.5 \times 10^{10}$ W/cm^2 [below threshold, Fig. 3(a)], the dipole oscillations grow initially and then saturate at a rather low level. Figure 3(c) shows the instantaneous laser frequency and the dipole frequency of the electron gas. The two frequencies stay close together initially, but then diverge for the below-threshold case.

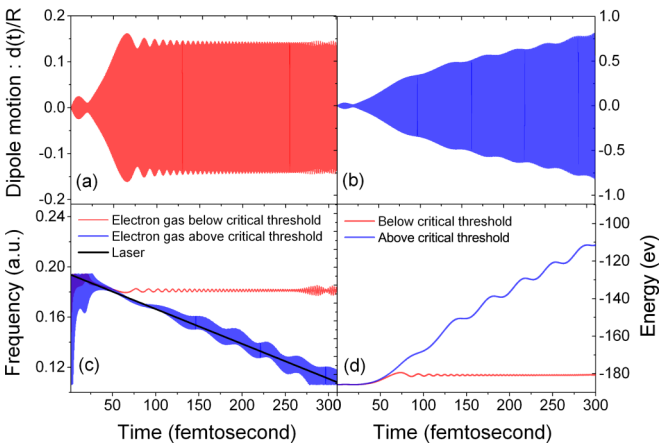

FIG. 3. (Color online) Autoresonant excitation of a gold nanoparticle with $N = 200$, for two values of the laser intensity, $I_0 = 4.5 \times 10^{10}$ W/cm^2 (below threshold, red curves) and $I_0 = 5.4 \times 10^{10}$ W/cm^2 (above threshold, blue curves). The top panels show the time evolution of the dipole $d(t)$ (a) below threshold and (b) above threshold. (c) Laser frequency (black straight line) and instantaneous dipole frequency of the electron gas for the below threshold (red) and above threshold (blue) cases. (d) Energy absorbed by the electron gas, for both cases.

In contrast, when $I_0 = 5.7 \times 10^{10}$ W/cm^2 (just above threshold), the amplitude of the dipole oscillations increases virtually without limits, reaching 80% of the size of the nanoparticle [Fig. 3(b)]. Thus, in practice, all the electrons have been ejected from the nanoparticle (although they are still accounted for by our dynamical model) on a time scale of the order of a few hundred femtoseconds. The laser and the electron gas frequencies are locked in resonance during the entire duration of the simulation [Fig. 3(c), blue line], which is the hallmark of the autoresonant excitation. This leads to strongly enhanced absorption of the laser energy by the nanoparticle, as is evident from the plot of the total absorbed energy in Fig. 3(d).

It must be noted that, since we expanded the Lagrangian in d/R, the force acting on the dipole in Eq. (8) becomes repulsive for d exceeding a certain value $d_{\max}$ (which depends on σ), thus making the model invalid for $d > d_{\max}$. This value reaches its minimum for $\sigma \approx \sigma_0$, where $d_{\max} \simeq 0.65R$. Even with this limitation, our simulations constitute a clear proof of principle that strongly nonlinear plasmon modes can be excited using an autoresonant laser pulse of relatively low intensity.

It is also interesting to compute the total power radiated by the electron gas, for cases above and below the critical threshold. Far from the nanoparticle, the electron gas can be viewed as an electric dipole of charge $-Ne$ and displacement $d(t)$ oscillating along the z axis. In this case we can apply the Larmor formula [45] for the total radiated power: $P(t) = e^2/(6\pi\epsilon_0 c^3)|\ddot{d}(t)|^2$.

Below threshold, the total power spectrum $P(\omega)$ is localized around the surface plasmon frequency [Fig. 4(a)]. In contrast, the spectrum is rich in high-order harmonics in the above-threshold regime [Fig. 4(b)], for which the electron gas explores the nonlinear part of the confining potential [46]. Such difference in the observed spectrum could be used as an experimental signature to assess the effectiveness of the autoresonant excitation. High-harmonic generation is also a crucial issue for the production and shaping of attosecond laser pulses [47].

Conclusion. We showed that by irradiating a metallic nanoparticle with an autoresonant chirped laser pulse, it is possible to drive the collective electron modes (surface

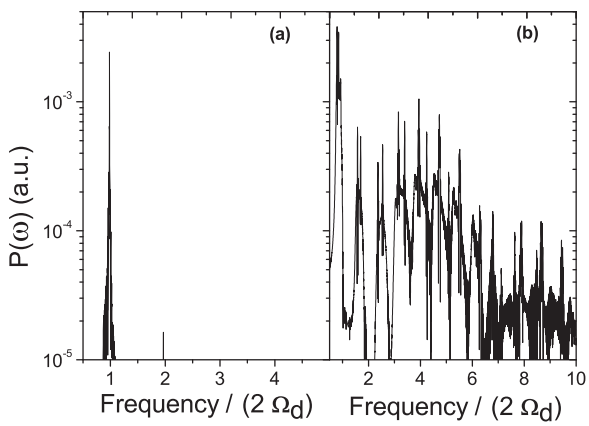

FIG. 4. Frequency spectrum of the total radiated power in a gold nanoparticle with $N = 200$, for two cases, below the autoresonance threshold (a) and above the threshold (b).

plasmons) far into the nonlinear regime, leading to enhanced energy absorbtion and complete ionization of the nanoparticle on a time scale of the order of 100 fs. Thanks to the autoresonant technique, the required laser intensity is rather modest ($\sim 10^{10}$ W/cm^2). Such enhanced absorption may be used, for instance, to improve the efficiency of nanoparticle-based radiotherapy [10].

The autoresonant mechanism is extremely flexible, since it requires no feedback as in usual control theory. Further, the laser does not need to be perfectly matched to the linear frequency (the only requirement is that the linear frequency be crossed during the excitation). This feature means that a whole assembly of nanoparticles [33] could be excited autoresonantly, even if they have different sizes and thus different plasmon resonances.

Acknowledgments. We thank the Agence Nationale de la Recherche, project Labex "Nanostructures in Interaction with their Environment," for financial support.

[1] U. Kreibig and M. Vollmer, *Optical Properties of Metal Clusters* (Springer, Berlin, 1995).
[2] J. A. Scholl, A. L. Koh, and J. A. Dionne, Nature (London) **483**, 421 (2012).
[3] Y. Luo, A. I. Fernandez-Dominguez, A. Wiener, S. A. Maier, and J. B. Pendry, Phys. Rev. Lett. **111**, 093901 (2013).
[4] M. S. Tame, K. R. McEnery, S. K. Özdemir, J. Lee, S. A. Maier, and M. S. Kim, Nature Phys. **9**, 329 (2013).
[5] S. Raza *et al.*, Nanophotonics **2**, 131 (2013).
[6] M. I. Stockman, Phys. Today **64**, 39 (2011).
[7] A. Moreau, C. Ciraci, J. J. Mock, R. T. Hill, Q. Wang, B. J. Wiley, A. Chilkoti, and D. R. Smith, Nature (London) **492**, 86 (2012).
[8] M.-C. Daniel and D. Astruc, Chem. Rev. **104**, 293 (2004).
[9] T. Endo *et al.*, Anal. Chem. **78**, 6465 (2006).
[10] J. F. Hainfeld, D. N. Slatkin, and H. M. Smilowitz, Phys. Med. Biol. **49**, N309 (2004).
[11] J.-Y. Bigot, V. Halté, J.-C. Merle, and A. Daunois, Chem. Phys. **251**, 181 (2000).
[12] C. Voisin, D. Christofilos, N. Del Fatti, F. Vallée, B. Prével, E. Cottancin, J. Lermé, M. Pellarin, and M. Broyer, Phys. Rev. Lett. **85**, 2200 (2000).
[13] W. Ekardt, Phys. Rev. B **31**, 6360 (1985).
[14] C. Guet and W. R. Johnson, Phys. Rev. B **45**, 11283 (1992).
[15] F. Calvayrac, P.-G. Reinhard, E. Suraud, and C. Ullrich, Phys. Rep. **337**, 493 (2000).
[16] T. V. Teperik, P. Nordlander, J. Aizpurua, and A. G. Borisov, Phys. Rev. Lett. **110**, 263901 (2013).
[17] O. Morandi, J. Phys. A: Math. Theor. **43**, 365302 (2010).
[18] R. Jasiak, G. Manfredi, and P.-A. Hervieux, New J. Phys. **11**, 063042 (2009).
[19] F. Haas, *Quantum Plasmas: An Hydrodynamic Approach* (Springer, Berlin, 2011).
[20] G. Manfredi and F. Haas, Phys. Rev. B **64**, 075316 (2001).
[21] M. Brewczyk, K. Rzazewski, and C. W. Clark, Phys. Rev. Lett. **78**, 191 (1997).
[22] A. Banerjee and M. K. Harbola, J. Chem. Phys. **113**, 5614 (2000).
[23] A. Domps, P.-G. Reinhard, and E. Suraud, Phys. Rev. Lett. **81**, 5524 (1998).
[24] G. Manfredi, P. A. Hervieux, and F. Haas, New J. Phys. **14**, 075012 (2012).
[25] C. Ciracì, J. B. Pendry, and D. R. Smith, Chem. Phys. Chem. **14**, 1109 (2013).
[26] N. Crouseilles, P.-A. Hervieux, and G. Manfredi, Phys. Rev. B **78**, 155412 (2008).
[27] F. Haas, G. Manfredi, P. K. Shukla, and P.-A. Hervieux, Phys. Rev. B **80**, 073301 (2009).
[28] J. Fajans and L. Friedland, Am. J. Phys. **69**, 1096 (2001).
[29] W. K. Liu, B. Wu, and J. M. Yuan, Phys. Rev. Lett. **75**, 1292 (1995).
[30] J. Fajans, E. Gilson, and L. Friedland, Phys. Rev. Lett. **82**, 4444 (1999).
[31] K. W. Murch *et al.*, Nature Phys. **7**, 105 (2011).
[32] G. Manfredi and P. A. Hervieux, Appl. Phys. Lett. **91**, 061108 (2007).
[33] C. N. Ramachandra Rao, G. U. Kulkarni, P. John Thomas, and P. P. Edwards, Chem. Soc. Rev. **29**, 27 (2000).
[34] A. D. Becke, Phys. Rev. A **38**, 3098 (1988).
[35] See Supplemental Material at http://link.aps.org/supplemental/10.1103/PhysRevB.89.161111 for all the details of the calculations (including electron correlations) and the raw numerical data.
[36] M. Kundu and D. Bauer, Phys. Rev. Lett. **96**, 123401 (2006).
[37] R. Esteban, A. G. Borisov, P. Nordlander, and J. Aizpurua, Nat. Commun. **3**, 825 (2012).
[38] G. Mie, Ann. Phys. (Leipzig) **330**, 377 (1908).
[39] C. Bréchignac, P. Cahuzac, J. Leygnier, and A. Sarfati, Phys. Rev. Lett. **70**, 2036 (1993).
[40] J. G. Aguilar *et al.*, Int. J. Quantum. Chem. **61**, 613 (1997).
[41] T. Reiners, C. Ellert, M. Schmidt, and H. Haberland, Phys. Rev. Lett. **74**, 1558 (1995).
[42] L. Brey, J. Dempsey, N. F. Johnson, and B. I. Halperin, Phys. Rev. B **42**, 1240 (1990).
[43] M. Madjet, C. Guet, and W. R. Johnson, Phys. Rev. A **51**, 1327 (1995).
[44] M. Maier, G. Wrigge, M. Astruc Hoffmann, P. Didier, and B. v. Issendorff, Phys. Rev. Lett. **96**, 117405 (2006).
[45] J. D. Jackson, *Classical Electrodynamics* (Wiley, New York, 1998).
[46] J. Nappa, G. Revillod, I. Russier-Antoine, E. Benichou, C. Jonin, and P. F. Brevet, Phys. Rev. B **71**, 165407 (2005).
[47] F. Krausz and M. Ivanov, Rev. Mod. Phys. **81**, 163 (2009).